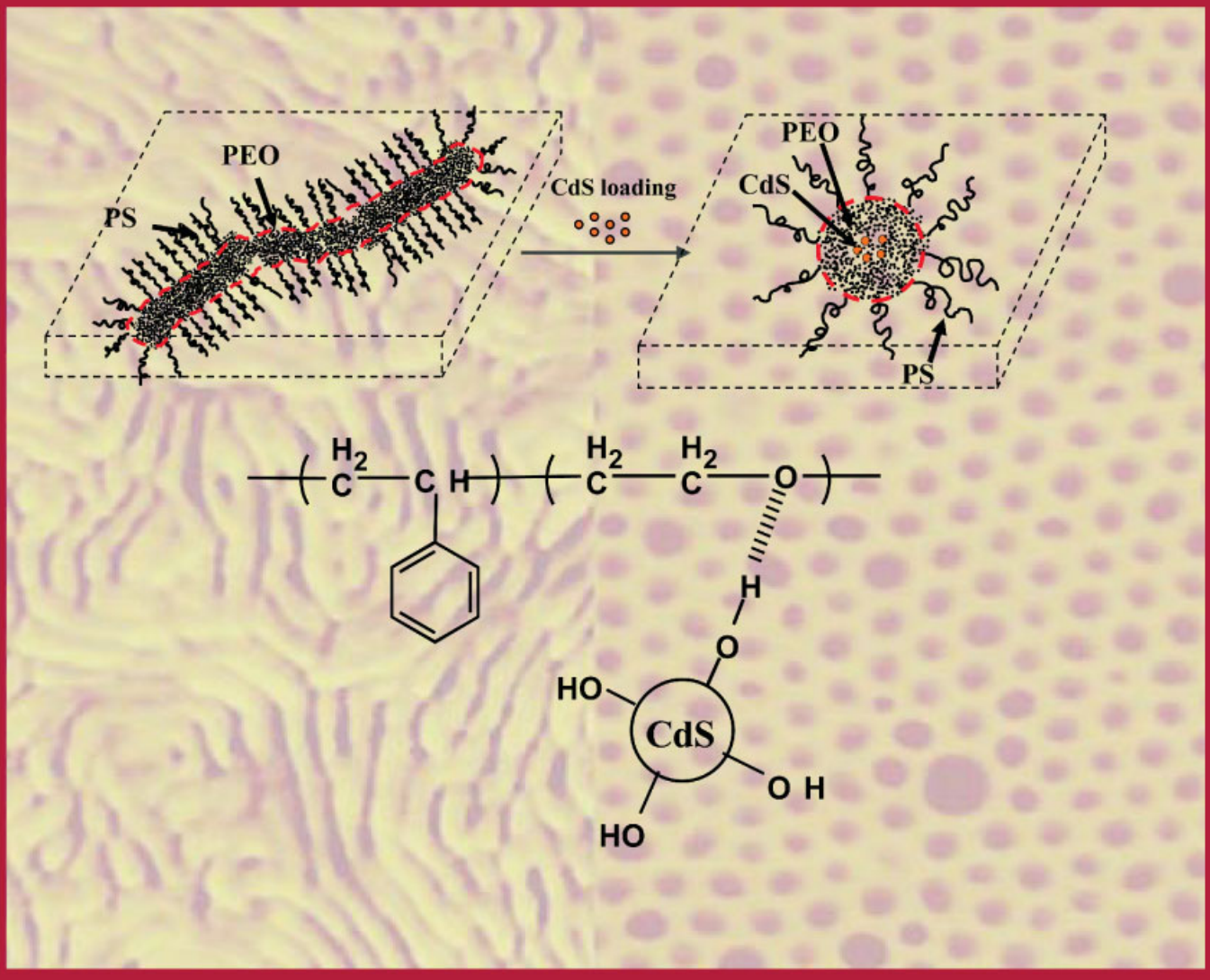

The Morphological Transformation from PEO Cylinders to CdS/PEO Spheres in Thin Films

©WILEY-VCH Macromolecular Rapid Communications

Summary: Polystyrene-*block*-poly(ethylene oxide) (SEO) block copolymer thin films, in which CdS clusters have been sequestered into the PEO domains of the SEO block copolymers, are found to induce the morphological transformation of PEO from cylinders to spheres, as shown by using atomic force microscopy (AFM), transmission electron microscopy (TEM), and scanning electron microscopy (SEM). This transformation is caused by the presence of hydrogen-bonding interactions between surface-hydroxylated CdS and PEO, as confirmed by nuclear magnetic resonance (NMR) studies.

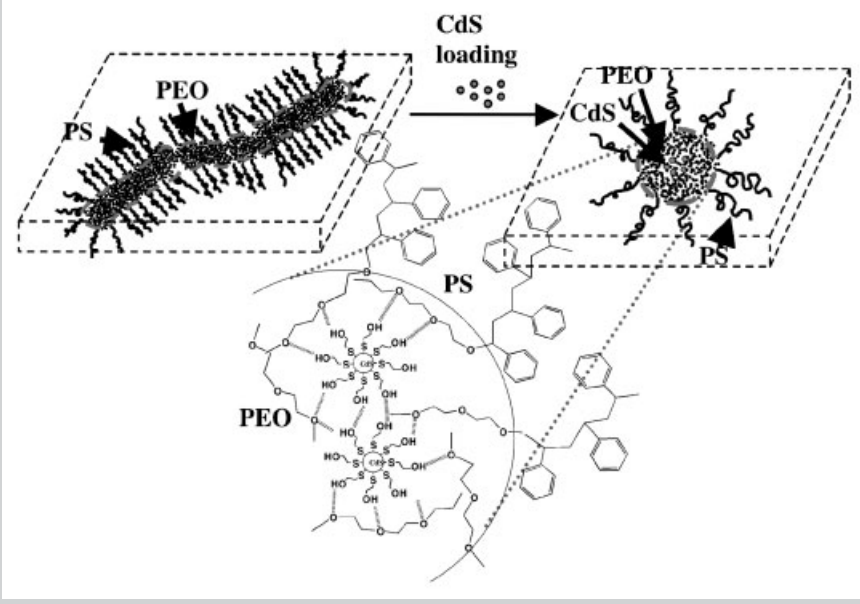

Morphological transformation of PEO cylinders into CdS/PEO spheres by hydrogen-bonding interactions between surface-hydroxylated CdS and PEO.

Effect of Surface-Hydroxylated CdS Nanoparticles on the Morphological Transformation of Polystyrene-*block*-Poly(ethylene oxide) Thin Films[a]

*Siao-Wei Yeh, Yao-Te Chang, Chia-Hung Chou, Kung-Hwa Wei**

Department of Materials Science and Engineering, National Chiao Tung University, Hsinchu, Taiwan 30049, ROC
Fax: (+886) 35-724727; E-mail: khwei@cc.nctu.edu.tw

Received: June 28, 2004; Revised: August 11, 2004; Accepted: August 12, 2004; DOI: 10.1002/marc.200400277

Keywords: block copolymers; cadmium sulfide; hydrogen bond; nanoparticles; polystyrene-*block*-poly(ethylene oxide)

Introduction

Block copolymers are versatile platform materials because they can self-assemble into various nanostructures with period thicknesses between 10 to 100 nm, under appropriate compositions and conditions, owing to microphase separation between incompatible blocks.[1–10] Hence, self-assembled block copolymers in a bulk form serve as good carriers for bringing nanoparticles into an ordered nanostructure.[11–15] More complicated block copolymer morphologies, involving the incorporation of nanoparticles into block copolymers, have been predicted by Balazs' group.[16]

[a] Supporting information for this article is available at the bottom of the article's abstract page, which can be accessed from the journal's homepage at http://www.mrc-journal.de, or from the author.

Previously, the selective sequestration of pre-synthesized surface-modified CdS and TiO_2 nanoparticles into one block of polystyrene-*block*-poly(ethylene oxide) (SEO) and polystyrene-*block*-poly(methyl methacrylate) (PS-*b*-PMMA) has been performed, respectively. The morphological transformation of bulk CdS/SEO with a higher molecular weight of SEO (PS/PEO = 125 000/1 610, volume fraction of PEO = 0.11) is also observed.[17a,17c] Moreover, the binding of nanoparticles to the PEO domains leads to spherical CdS/PEO domains with a greatly enhanced thermal stability.[17b]

On the other hand, diblock copolymer thin films (less than 100 nm) can be used to control the spatial position of nanoparticles using nanostructured block copolymers by synthesizing the nanocrystal clusters within microphase-separated domains. Using a polystyrene-*block*-polyvinylpyridine (PS-*b*-PVP) micellar solution, ordered Au clusters,[18] Co and Fe arrays,[19] and self-assembly of both Au and Fe_2O_3 nanoparticles,[20] have all been synthesized. High density nanostructures of silicon nitride, GaAs,[21] Au/Cr,[22a] and magnetic cobalt dots[23] have been fabricated using block copolymers as lithographic templates. Au, Ag,[24] and magnetic Co[22b] nanowires can also be produced using a PS-*b*-PMMA block copolymer template. Recently, Russell and co-workers were able to screen different sizes of pre-synthesized CdSe nanoparticles with a nanoporous PS-*b*-PMMA template by capillary force.[25] Schrock and co-workers sequestered CdSe nanoclusters within phosphine-containing domains of a diblock copolymer.[26] In this study, we prepare CdS/SEO thin films, with CdS clusters sequestered in the PEO domains of the SEO block copolymer, and investigate the effects of hydrogen bonding between surface-hydroxylated CdS and ethylene oxide on the morphological transformation of CdS/SEO thin films from cylindrical PEO structures into spherical CdS/PEO domains, as shown in Scheme 1. The method of preparing CdS/SEO thin films in this study has been submitted elsewhere.[27]

Experimental Part

The SEO diblock copolymer ($\overline{M}_{w,PS}/\overline{M}_{w,PEO}$ = 19 000/12 600) were obtained from Polymersource, Inc. ^{1}H NMR ((D_8)-toluene): δ = 7.28–6.84 (m, H^4 and H^5), 6.64 (d, H^3, $J_{3,4}$ = 19.35 Hz), 3.50 (s, H^6), 2.07 (s, H^2),1.563 (s, H^1). CdS nanoparticles were synthesized by reacting cadmium acetate dihydrate ($Cd(Ac)_2 \cdot 2\ H_2O$) and sodium sulfide (Na_2S) with mercaptoethanol (HSC_2H_4OH) as a surfacant, following a modification of the kinetic trapping method.[28] The average size of these CdS nanoparticles in *N*,*N*-dimethylforamide (DMF) is approximately 2.5 nm. Proper ratios of CdS and SEO were mixed in DMF because DMF is a good solvent for surface-hydroxylated CdS and PEO domains of SEO block copolymers. After removing DMF under vacuum at 323 K and

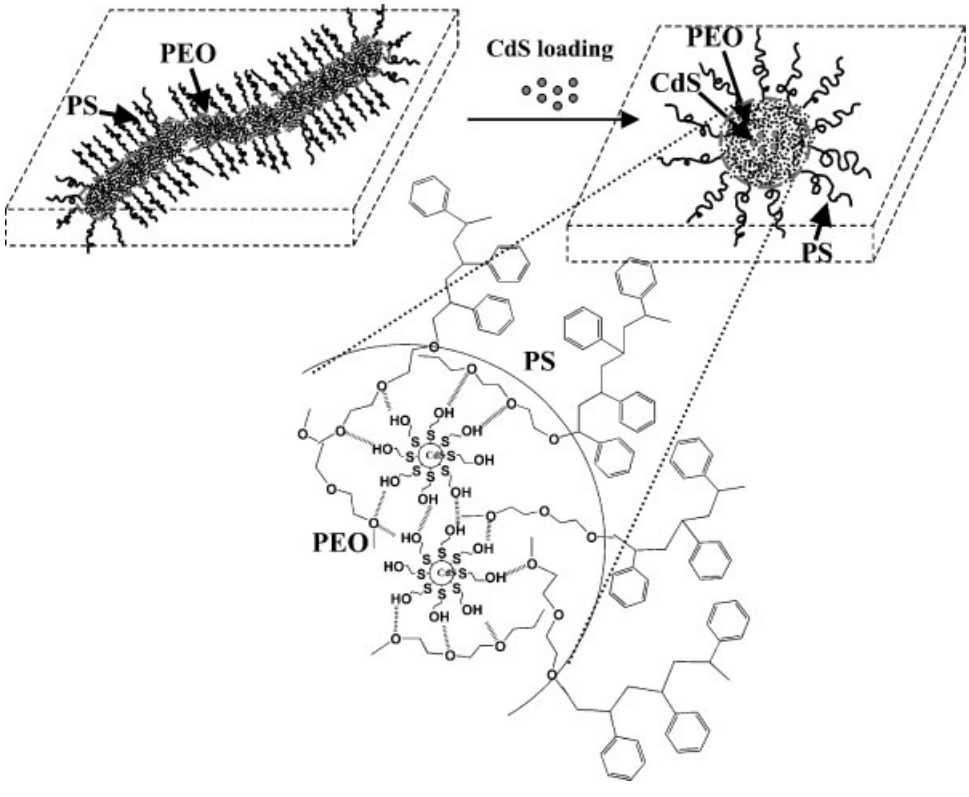

Scheme 1. Morphological transformation of PEO cylinders into CdS/PEO spheres by hydrogen-bonding interactions between surface-hydroxylated CdS and PEO.

maintaining at 383 K for 24 h, the bulk CdS/SEO nanocomposites were formed. The CdS nanoparticles in each PEO domain are defined as a CdS cluster in this study. To sequester CdS clusters into the PEO domains and fabricate CdS/SEO thin films (see also Supporting information), toluene is used to prepare 1% CdS/SEO micellar solutions with CdS/PEO-core and PS-shell micellar structures in solution by solvent selectivity, because toluene is a good solvent for PS but a poor one for PEO. The micellar solutions were then spin-coated at 5 000 rpm for 60 s onto carbon-coated silicon wafers. After drying, the CdS/SEO thin films were characterized by atomic force microscopy (AFM), transmission electron microscopy (TEM), and scanning electron microscopy (SEM). AFM measurements were performed with a Digital Nanoscope IIIa. TEM samples of monolayer-thin films on carbon-coated silicon wafers were prepared by removing the film from the wafer with 1% HF solution and depositing it on a copper net. TEM images were obtained with an Hitachi H-600 microscope. SEM images were obtained with a thermal field emission scanning electron microscope (JSM-6500F). ^{1}H NMR and two-dimensional ^{1}H-^{13}C NMR spectra for hydrogen bonding studies were recorded on a Varian Unity-300 MHz NMR spectrometer by using (D_8)toluene as the solvent.

Results and Discussion

Figure 1(a–d) show phase contrast AFM images and TEM images of approximately 40-nm thick SEO thin films containing different amounts of CdS nanoparticles on carbon-coated silicon wafers. Figure 1(e) shows an SEM cross-sectional image of 28 wt.-% CdS nanoparticles in an SEO thin film on the silicon wafer after immersion in water. In the phase contrast AFM images, dark and light regions represent amorphous PEO and PS domains,[2] respectively, because of the difference in the viscoelastic response of these materials. In TEM images of pure SEO without staining, however, PEO and PS domains are revealed as bright and dark regions, respectively, because of the greater electron density in styrene. In Figure 1(a), the pure SEO thin film consists of PEO cylinders, 18 nm in diameter, dispersed in a PS matrix. This morphology is largely determined by the volume fraction of the PEO block. The average length of PEO cylinders is larger than 300 nm. Moreover, the PEO domain of the SEO thin films is not crystalline, because of the difference in viscoelastic properties shown in the AFM image of Figure 1(a).[2] In Figure 1(b), the presence of 7 wt.-% CdS induces a small fraction of PEO domains to become spherical, as seen in the AFM image; the majority of PEO domains, however, remain cylindrical in shape, with lengths ranging from 200 to 300 nm. A close examination of the PEO domains shows that dark CdS clusters are selectively dispersed in the spherical PEO domains, with PEO cylinders remaining in a pure state. The average size of the PEO cylinders and CdS/PEO spheres in the CdS/SEO thin films

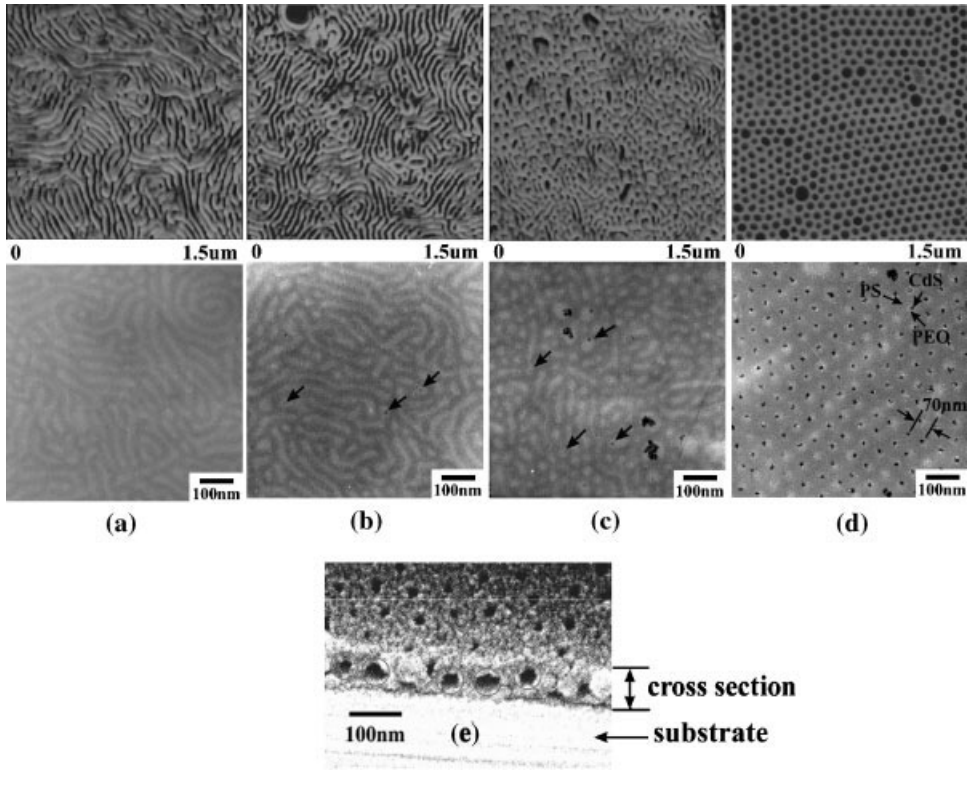

Figure 1. Phase contrast AFM images and TEM images of 40-nm thick CdS/SEO thin films with (a) 0, (b) 7, (c) 14, and (d) 28 wt.-% CdS content after spin-coating onto carbon-coated silicon wafers. (e) The SEM cross-sectional image of 28 wt.-% CdS nanoparticles in SEO thin films.

Table 1. The percentage and average length of PEO cylinders, the percentage of CdS/PEO spheres (CdS/PEO spheres-%), and the percentage of shifted CH_2O protons in PEO (shifted CH_2O-%) that appear in CdS/SEO thin films of various CdS content.

Film	PEO cylinders			CdS/PEO Spheres	Shifted CH_2O
	%[a)]	Average length	Diameter	%[b)]	%[c)]
		nm	nm		
Pure SEO	>97	>300	18	<3	0
7 wt.-% CdS/SEO	71	200–300	17	29	29.1
14 wt.-% CdS/SEO	33	80–150	15	67	62.3
28 wt.-% CdS/SEO	0	–	–	100	84.4

[a)] The percentage of PEO cylinders is calculated by the ratio of $\frac{A_{PEO}}{A_{PEO}+A_{CdS/PEO}}$ from AFM and TEM images.

[b)] The percentage of CdS/PEO spheres is calculated by the ratio of $\frac{A_{CdS/PEO}}{A_{PEO}+A_{CdS/PEO}}$ from AFM and TEM images.

[c)] The percentage of shifted CH_2O protons in PEO is derived from the integration of ^1H NMR curves.

with various CdS contents are given in Table 1. The average fractions of PEO cylinders and CdS/PEO spheres are also listed. In Figure 1(c), more spherical CdS/PEO domains appear when 14 wt.-% CdS nanoparticles are incorporated. The average length of the PEO cylinders shrinks to between 80 to 150 nm, with a diameter of approximately 15 nm, which is shorter and thinner than that of the PEO cylinders in pure SEO. Figure 1(d) shows that as the CdS content increases to 28 wt.-%, CdS-included PEO domains completely transform into a spherical morphology, as determined by AFM imaging and TEM, where the majority of CdS-incorporated spherical PEO domains are observed to form arrays. The size of spherical CdS/PEO domains is approximately 40 to 50 nm, and the intersphere distance is approximately 70 nm. The CdS/PEO spherical morphology is confirmed by examining a cross-sectional image of the 28 wt.-% CdS/SEO thin film (ca. 100-nm thick), which has been immersed in water and sectioned in liquid nitrogen. Because the CdS/PEO domains are soluble in water, round holes appear in the cross-sectional SEM image of the 100-nm thick, 28 wt.-% CdS/SEO film, indicating that the shape of CdS/PEO domains are indeed spherical and not oriented cylinders perpendicular to the surface. By comparing the AFM, TEM, and SEM results of the 28 wt.-% CdS/SEO film, we can deduce that the CdS clusters act as some kind of spherical site in the center of the CdS/PEO domains leading to ''spherical double-brushes'' with a CdS cluster core, a first PEO corona covered by an outer PS corona which also forms the matrix into which the CdS/PEO spherical domains are embedded. The morphological transformation from cylindrical PEO into spherical CdS/PEO domains can be observed clearly when loading the surface-hydroxylated CdS. To verify that the morphological transformation of CdS/SEO thin films is caused by the presence of the surface-hydroxylated CdS nanoparticles, a control experiment with the same process of thin film preparation was carried out, in which only surfactant, mercaptoethanol, was added to SEO; no morphological change was observed to occur. The main cause of this morphological transformation might be attributable to a strong interaction between the hydroxyl groups on the surface of CdS clusters and the PEO domains.

The interaction between mercaptoethanol ligands on CdS and the PEO blocks is attributed to dipole–dipole or hydrogen-bonding interactions, which can be investigated by nuclear magnetic resonance (NMR) spectroscopy. Figure 2 shows ^1H NMR spectra for different amounts of CdS nanoparticles in SEO in (D_8)toluene; in curve (e), the spectrum of D_2SO_4 in SEO in (D_8)toluene has been normalized using the PS peaks at 1.56 and 6.67 ppm as the standard and the same solid content in (D_8)toluene. In Figure 2(a), the 1H NMR spectra of pure SEO solution in (D_8)toluene, broad peaks at approximately 1.56, 2.05, and 6.40–7.20 ppm all correspond to protons in the PS block, and the sharp peaks at approximately 2.08, 7.00, 7.01, and 7.09 ppm are all attributed to protons in (D_8)toluene. The narrow peak at approximately 3.49 ppm is assigned to protons in the CH_2 group next to oxygen in the PEO block. The presence of CdS in the PEO block in curves (b)–(d), which are enlarged portions of the spectra of CdS/SEO, cause the CH_2O peak for PEO at 3.49 ppm to reduce in size; a broad new peak at 4.09 ppm emerges as the CdS content in PEO increases. To identify this new peak, a two-dimensional ^{13}C-^1H NMR experiment for 14 wt.-% CdS/SEO was performed. Figure 2(f) displays this spectrum, which contains the broad new peak at approximately 4.09 ppm for the protons in CH_2O groups in PEO, in place of the original peak at 3.49 ppm for pure SEO. Moreover, the sum of the areas under the peaks at 3.49 and 4.09 ppm in each CdS/SEO NMR spectrum is almost equal to the area of the peak at 3.49 ppm in the pure SEO spectrum. These two facts suggest that the broad new peak at 4.09 ppm is because of a shift of the peak at 3.49 ppm. In order to elucidate the cause, reversible heating and cooling experiments were carried out on the samples. Figure 2(g) shows NMR spectra of 14 wt.-% CdS/SEO in (D_8)toluene at 21 and 60 °C. For 14 wt.-% CdS/SEO heated to 60 °C in (D_8)toluene solution, the shifted CH_2O peak for CdS/PEO disappears, and the integral peak area at

3.49 ppm in the spectra observed at 60 °C is restored, as shown in curve (g). Hydrogen bonding between CdS clusters and PEO in CdS/SEO nanocomposites can explain this behavior, since hydrogen bonds are destroyed at elevated temperatures.[29] Moreover, curve (e) shows a similar shift for the CH_2O group in PEO after protonation by the addition of D_2SO_4 in pure SEO/(D_8)toluene solution, which indicates that the shift of the CH_2O group in PEO may be caused by hydrogen bonding. Therefore, the broad and shifted CH_2O peak indicates that CdS nanoparticles interact with the PEO block by strong intermolecular forces (i.e., hydrogen bonding between the hydroxyl groups of CdS

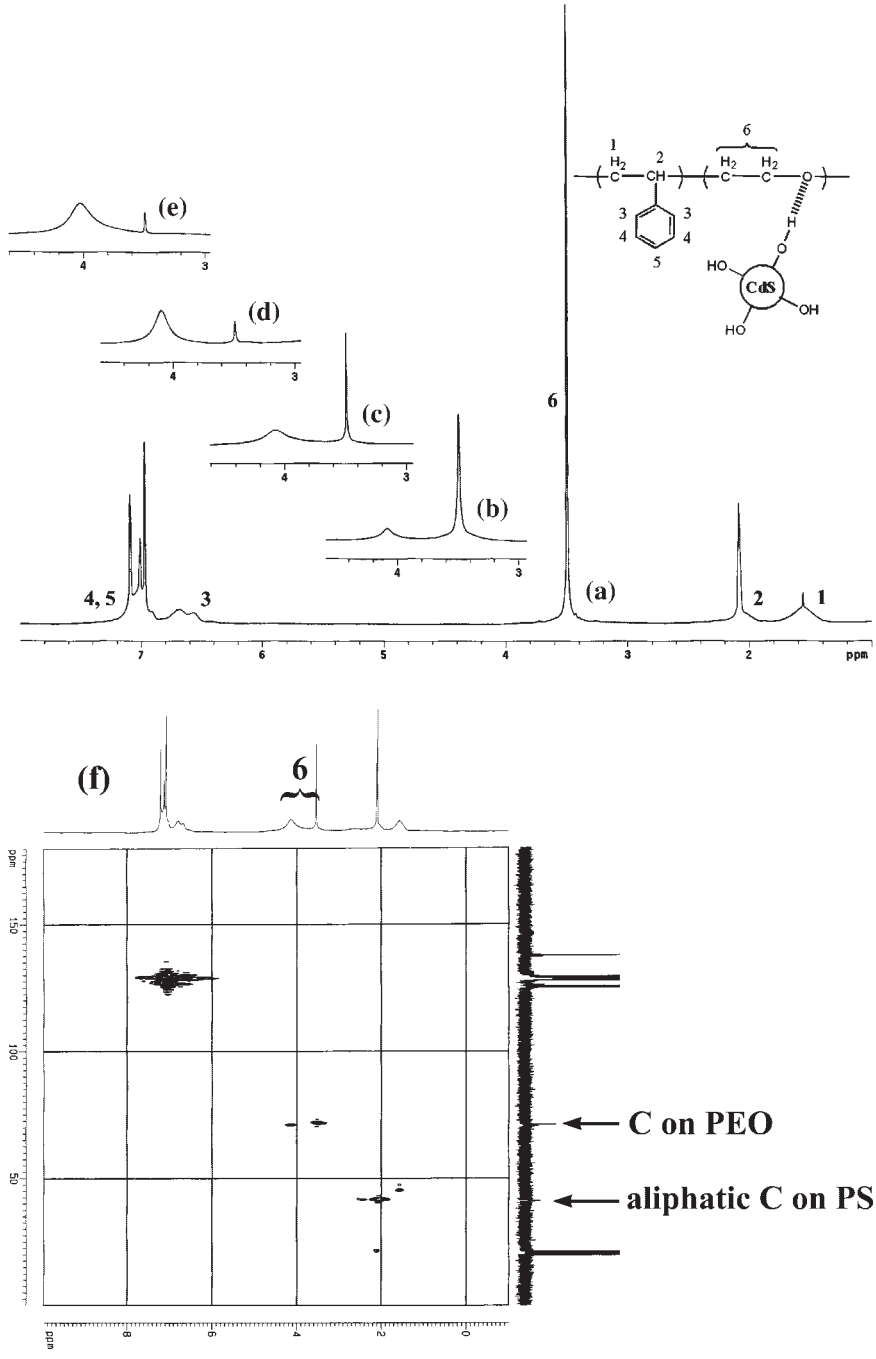

Figure 2. ^{1}H NMR spectra of (a) 0, (b) 7, (c) 14, and (d) 28 wt.-% CdS/SEO, and (e) D_2SO_4 in SEO in (D_8)toluene after normalization. (f) A two-dimensional ^{13}C-^{1}H NMR spectrum of 14 wt.-% CdS/SEO. (g) NMR spectra of 14 wt.-% CdS/SEO at different temperatures (21 and 60 °C).

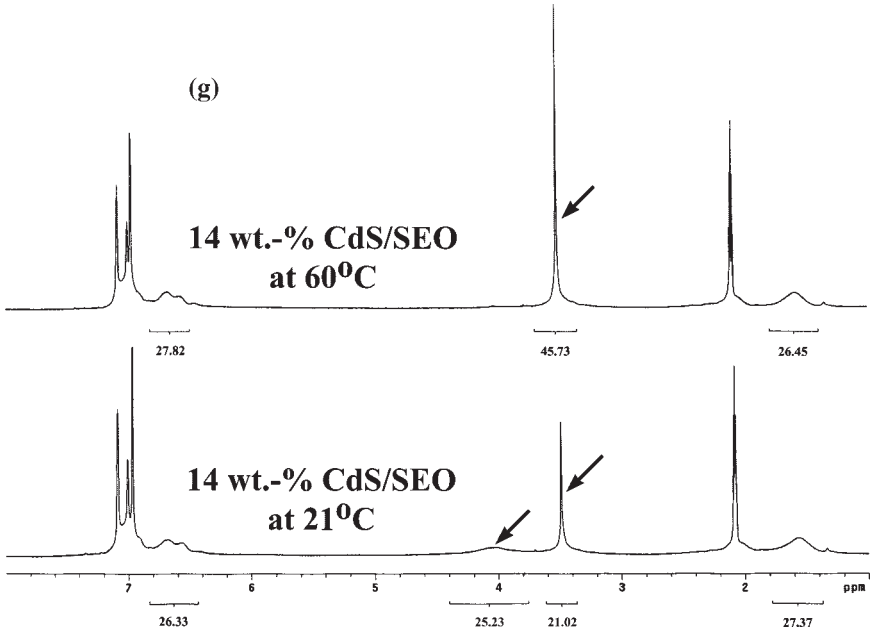

Figure 2. (*Continued*)

and the oxygen of PEO). This interaction changes the microenvironment around the CH_2O groups in PEO, resulting in the morphological transformation from cylindrical PEO domains to spherical CdS/PEO domains.

Hence, the morphological transformation brought on by the incorporation of mercaptoethanol-modified CdS nanoparticles can be explained by hydrogen bonding. In the composite CdS/SEO system, two types of hydrogen bonding are involved. The first, as demonstrated in NMR studies, occurs between the free hydroxyl groups on CdS and the oxygen of PEO, which results in the segregation of CdS in PEO, a change in the surface energy of CdS/PEO domains, and a morphological transformation from PEO cylinders to CdS/PEO spheres. The other interaction is attributable to mutual hydrogen bonding between surface-hydroxylated CdS nanoparticles, which causes them to self-aggregate. Therefore, the PEO chains that surround the CdS clusters form CdS/PEO spheres, and CdS nanoparticles aggregate in the PEO domains, as shown in Scheme 1. Comparisons between the percentage of shifted CH_2O protons in PEO (two lines of solid dots) and the percentage of CdS/SEO morphological spheres (white hollow squares) for various CdS content is presented in Table 1 and Figure 3. When the content of CdS is low (ca. 0–14 wt.-%), the percentages of both shifted CH_2O protons in PEO (ca. 0–62.3%) and CdS/SEO spheres (ca. 3–67%), which depend linearly on CdS content, show the same trace. This indicates that CdS is scarce in the PEO domains for low CdS content. For high CdS content (28 wt.-%), all CdS/PEO domains are spheres in the thin film morphology, but only 84.4% of PEO chains connect to CdS, a result that is not linearly dependent on CdS content. This indicates that more CdS nanoparticles clump together instead of connecting to PEO chains when the CdS content is high (28 wt.-%), and the remaining 15.6% exist as free ethylene oxide units present between CdS nanoparticles, or are near the interface between PS and PEO domains.

Conclusion

The morphological transformation from PEO cylinders to spheres in thin films, induced by the incorporation of CdS nanoparticles, is clearly observed in AFM, TEM, and SEM images. The transformation is explained by hydrogen-bonding interactions between surface-hydroxylated CdS and PEO, as demonstrated by NMR studies. Hydrogen

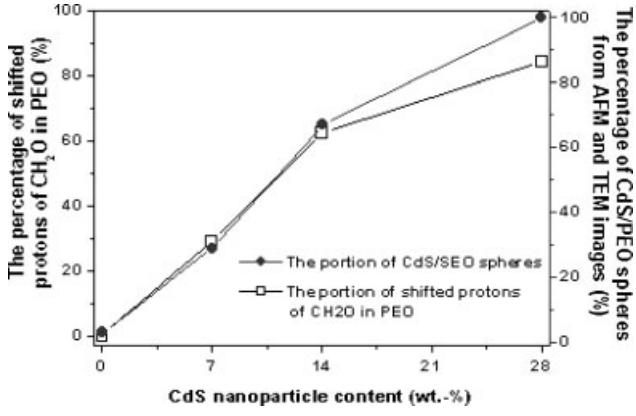

Figure 3. The comparisons between the percentage of shifted CH_2O protons in PEO (solid dots) and the percentage of CdS/SEO morphological spheres (empty squares) for various CdS contents.

bonding changes the chemical environment of the PEO next to the CdS clusters. In the case of 28 wt.-% CdS/SEO thin films, the ordered arrangement of CdS clusters is fabricated by an SEO block copolymer template.

Acknowledgements: The authors acknowledge the *National Science Council* and the *US Air Force Office of Scientific Research* for funding this work through NSC 91-2120-M-009-001 and AOARD-03-4018, respectively.

[1] F. S. Bates, *Science* **1991**, *251*, 898.
[2] G. Reiter, G. Castelein, J.-U. Sommer, A. Rollele, T. Thurn-Albrecht, *Phys. Rev. Lett.* **2001**, *87*, 226101.
[3] L. Li, Y. Serero, M. H. J. Koch, W. H. de Jeu, *Macromolecules* **2003**, *36*, 529.
[4] S. Jiang, A. Gopfert, B. Abetz, *Macromolecules* **2003**, *36*, 6171.
[5] L. Zhu, S. Z. D. Cheng, P. Huang, Q. Ge, R. P. Quirk, E. L. Thomas, B. Lotz, B. S. Hsiao, F. Yeh, L. Liu, *Adv. Mater.* **2002**, *14*, 31.
[6] R. A. Segalman, A. Hexemer, E. J. Kramer, *Phys. Rev. Lett.* **2003**, *91*, 196101.
[7] S. Choi, K. M. Lee, C. D. Han, N. Sota, T. Hashimoto, *Macromolecules* **2003**, *36*, 793.
[8] E. Buck, J. Fuhrmann, *Macromolecules* **2001**, *34*, 2172.
[9] D. Sundrani, S. B. Darling, S. J. Sibener, *Nano Lett.* **2004**, *4*, 273.
[10] N. Rehse, A. Knoll, R. Magerle, G. Krausch, *Macromolecules* **2003**, *36*, 3261.
[11] S. Forster, M. Antonietti, *Adv. Mater.* **1998**, *10*, 195.
[12] M. Lazzari, M. A. Lopez-Quintela, *Adv. Mater.* **2003**, *19*, 1583.
[13] C. Park, J. Yoon, E. L. Thomas, *Polymer* **2003**, *44*, 6725.
[14] I. W. Hamley, *Nanotechnology* **2003**, *14*, R39.
[15] M. R. Bockstaller, Y. Lapentnikov, S. Margel, E. L. Thomas, *J. Am. Chem. Soc.* **2003**, *125*, 5276.
[16] [16a] J. Y. Lee, R. B. Thompson, D. Jasnow, A. C. Balazs, *Macromolecules* **2002**, *35*, 4855; [16b] J. Y. Lee, A. C. Balazs, R. B. Thompson, R. M. Hill, *Macromolecules* **2004**, *37*, 3536.
[17] [17a] S. W. Yeh, K. H. Wei, Y. S. Sun, U. S. Jeng, K. S. Liang, *Macromolecules* **2003**, *36*, 7903; [17b] U. S. Jeng, Y. S. Sun, H. Y. Lee, C. H. Hsu, K. S. Liang, S. W. Yeh, K. H. Wei, *Macromolecules* **2004**, *37*, 4617; [17c] C. C. Weng, K. H. Wei, *Chem. Mater.* **2003**, *15*, 2936.
[18] M. Haupt, S. Miller, R. Glass, M. Arnold, R. Sauer, K. Thonke, M. Moller, J. P. Spatz, *Adv. Mater.* **2003**, *15*, 829.
[19] J. I. Abes, R. E. Cohen, C. A. Ross, *Chem. Mater.* **2003**, *12*, 1125.
[20] B. H. Sohn, J. M. Choi, S. Yoo, S. H. Yun, W. C. Zin, J. C. Jung, M. Kanehara, T. Hirata, T. Teranishi, *J. Am. Chem. Soc.* **2003**, *125*, 6368.
[21] M. Park, C. Harrison, P. M. Chaikin, R. A. Register, D. H. Adamson, *Science* **1997**, *276*, 1401.
[22] [22a] K. Shin, K. A. Leach, J. T. Goldbach, D. H. Kim, J. Y. Jho, M. Tuominen, C. J. Hawker, T. P. Russell, *Nano Lett.* **2002**, *2*, 933; [22b] M. Bal, A. Ursache, M. Tuominen, J. T. Goldbach, T. P. Russell, *Appl. Phys. Lett.* **2002**, *81*, 3479.
[23] J. Y. Cheng, C. A. Ross, V. Z.-H. Chan, E. L. Thomas, R. G. H. Lammertink, G. J. Vancso, *Adv. Mater.* **2001**, *13*, 1174.
[24] W. A. Lopes, H. M. Jaeger, *Nature* **2001**, *414*, 735.
[25] M. J. Misner, H. Skaff, T. Emrick, T. P. Russell, *Adv. Mater.* **2003**, *15*, 221.
[26] D. E. Fogg, L. H. Radzilowski, R. Blanski, R. R. Schrock, E. L. Thomas, *Macromolecules* **1997**, *30*, 417.
[27] S. W. Yeh, T. L. Wu, K. H. Wei, *Nano Lett.*, submitted.
[28] [28a] J. G. C. Veinot, M. Ginzburg, W. J. Pietro, *Chem. Mater.* **1997**, *9*, 2117; [28b] N. Herron, Y. Wang, H. Eckert, *J. Am. Chem. Soc.* **1990**, *112*, 1322.
[29] M. J. Kunz, G. Hayn, R. Saf, W. H. Binder, *J. Polym. Sci., Part A: Polym. Chem.* **2004**, *42*, 661.

